# Preparation and Characterization of Gold Nanoshells Coated with Self-Assembled Monolayers

Tan Pham,[†] Joseph B. Jackson,[‡] Naomi J. Halas,[‡] and T. Randall Lee*,[†]

*Department of Chemistry, University of Houston, Houston, Texas 77204-5003, and Department of Electrical and Computer Engineering, Rice University, Houston, Texas 77005*

*Received September 3, 2001. In Final Form: April 1, 2002*

This paper describes the functionalization of the surfaces of gold nanoshells, which consist of silica nanoparticles coated with a continuous thin layer of gold. Previous studies have shown that gold nanoshells exhibit optical properties similar to those of metal colloids (e.g., strong optical absorptions and large third-order nonlinear optical polarizabilities). In contrast to metal colloids, however, the plasmon resonance of the nanoshells can be tuned to specific wavelengths across the visible and infrared range of the electromagnetic spectrum by adjusting the relative size of the dielectric core and the thickness of the gold overlayer. In efforts to develop new strategies for protecting and manipulating these nanoparticles, this paper describes the functionalization of the surfaces of gold nanoshells with self-assembled monolayers derived from the adsorption of a series of alkanethiols. The nanoshells are characterized by transmission electron microscopy, UV−vis spectroscopy, FTIR spectroscopy, Raman spectroscopy, and X-ray photoelectron spectroscopy and by examining their relative solubility in a variety of organic solvents.

## Introduction

Much recent research has focused on the fabrication of new types of nanoparticles, particularly those with optical and electrical properties that can be controlled with precision.[1−3] Nanoparticles derived from noble metals have received particular attention because of their stability and their ease of preparation.[2,4] Recently, Halas and co-workers reported a new hybrid nanoparticle system that consists of a dielectric core surrounded by a thin noble metal shell.[1,2] These nanoparticles, termed "nanoshells", possess unique optical properties, including a strong optical absorbance and a large third-order nonlinear optical susceptibility. Perhaps more importantly, the absorbance can be selectively tuned to any wavelength across the visible and infrared regions of the spectrum simply by adjusting the ratio of the dielectric core to the thickness of the metal overlayer. These features render nanoshells attractive for use in technologies ranging from conducting polymer devices to biosensing and drug delivery.[5−7] Currently, there exists a need for the development of new strategies for protecting and manipulating these nanoparticles in order to expand their realm of use.

At present, the most versatile nanoshell system is based on the coating of silica nanoparticles with a thin layer of gold.[2] Scheme 1 shows the typical strategy used to prepare these gold nanoshells. A silica nanoparticle core is treated with an amine-terminated surface silanizing agent (e.g., 3-aminopropyltrimethoxysilane, APTMS). The resultant

**Scheme 1. Strategy Used To Grow a Gold Nanoshell around a Silica Nanoparticle Core**

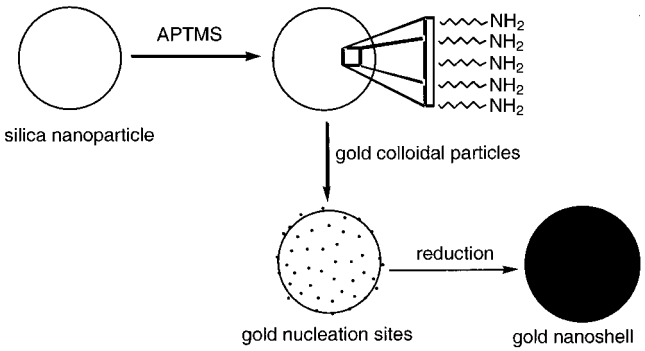


terminal amine groups[8−10] act as attachment points for small colloidal gold particles, which then serve as nucleation sites for the coalescence of the thin gold overlayer. We chose silica nanoparticles as the dielectric cores not only because methods for the functionalization of the surface of silica are well-known[8] but also because colloidal silica particles can be prepared with reproducibly spherical shapes and narrow size distributions.[11]

The synthesis of gold colloid typically involves the reduction of gold salts in the presence of surfactants or other stabilizers.[9,12−17] Of all possible strategies, the reduction of chloroauric acid with tetrakis(hydroxymethyl)phosphonium chloride (THPC) affords relatively small gold particles (e.g., 2 nm) with a net negative interfacial charge.[9] While these small colloidal particles can attach to APTMS-functionalized silica cores by coordinating to the lone pairs of the terminal amine groups, the attachment can be enhanced perhaps severalfold by electrostatic

[†] University of Houston.

[‡] Rice University.

(1) Averitt, R. D.; Sarkar, D.; Halas, N. J. *Phys. Rev. Lett.* **1997**, *78*, 4217.

(2) Oldenberg, S. J.; Averitt, R. D.; Westcott, S. L.; Halas, N. J. *Chem. Phys. Lett.* **1998**, *288*, 243.

(3) Haynes, C. L.; Van Duyne, R. P. *J. Phys. Chem. B* **2001**, *105*, 5599.

(4) Hieminz, P. C. *Principles of Colloid and Surface Chemistry*; Marcel Dekker: New York, 1986.

(5) Hale, G. D.; Jackson, J. B.; Shmakova, O. E.; Lee, T. R.; Halas, N. J. *Appl. Phys. Lett.* **2001**, *78*, 1502.

(6) West, J. L.; Halas, N. J. *Curr. Opin. Biotechnol.* **2000**, *11*, 215.

(7) Sershen, S. R.; Westcott, S. L.; Halas, N. J.; West, J. L. *J. Biomed. Mater. Res.* **2000**, *51*, 293.

(8) Ulman, A. *An Introduction to Ultrathin Organic Films*; Academic: New York, 1991.

(9) Grabar, K. C.; Allison, K. J.; Baker, B. E.; Bright, R. M.; Brown, K. R.; Freeman, R. G.; Fox, A. P.; Keating, C. D.; Musick, M. D.; Natan, M. J. *Langmuir* **1996**, *12*, 2353.

(10) Sato, T.; Brown, D.; Johnson, B. F. G. *J. Chem. Soc., Chem. Commun.* **1997**, 1007.

(11) Stöber, W.; Fink, A.; Bohn, E. *J. Colloid Interface Sci.* **1968**, *26*, 62.

10.1021/la015561y CCC: $22.00 
Published on Web 05/17/2002

effects, wherein the negatively charged THPC gold nanoparticles are attracted to the amine groups, which are positively charged at the pH used for the attachment process.[18] This strategy leads to silica nanoparticles in which ~25% of the surface is covered by colloidal gold particles that can be used to nucleate the growth of the gold overlayer.[18−22]

After growth of the gold overlayer, we wished to coat the exposed metal surface with a self-assembled monolayer (SAM), which can be spontaneously generated by treatment with alkanethiols or alkyl disulfides.[23,24] We believed that the functionalization of nanoshells with SAMs would facilitate nanoshell purification and offer new strategies for nanoshell manipulation in subsequent investigations and/or applications. Furthermore, independent studies have shown that the coating of noble metal surfaces with SAMs reduces corrosion and promotes stability of the metal interface.[25−27] Recent work involving the surface functionalization of metal colloids has focused on the adsorption of organic molecules onto the surfaces of gold, silver, copper, and platinum nanoparticles.[23−33] These functionalized metal colloids have found uses in the fabrication of materials for microelectronics,[34] electrodes,[35] catalysis,[34] and labeling and monitoring devices.[36] SAM-coated metal nanoparticles are insensitive to air and moisture and are soluble in a wide range of organic solvents.[24]

In this paper, we describe the preparation of gold nanoshells and the subsequent functionalization of the nanoshell surface with three separate alkanethiols of increasing chain length: dodecanethiol, hexadecanethiol, and octadecanethiol. We characterize the nanoshells by using transmission electron microscopy (TEM), Fourier transform infrared (FTIR) spectroscopy, Raman spectroscopy, X-ray photoelectron spectroscopy (XPS), and ultraviolet−visible (UV−vis) spectroscopy and by examining their solubilities in a variety of common solvents.

## Experimental Section

**Materials.** All reagents were purchased from the indicated suppliers and used without further purification: tetraethyl orthosilicate, tetrakis(hydroxymethyl)phosphonium chloride, sodium borohydride, 3-aminopropyltrimethoxysilane, 1-dodecanethiol, 1-hexadecanethiol, and 1-octadecanethiol (all from Aldrich); sodium hydroxide, ammonium hydroxide, and formaldehyde (all from EM Sciences); hydrogen tetrachloroaurate-(III) hydrate (Strem); and potassium carbonate (J. T. Baker). Similarly, all solvents were used as received from the indicated suppliers: HPLC grade water, tetrahydrofuran, pentane, hexane, benzene, and dicholoromethane (all from EM Sciences); carbon tetrachloride (Aldrich); and absolute ethanol (McKormick Distilling Co.).

**Characterization Methods.** To collect the TEM images, we used a JEOL JEM-2010 electron microscope operating at a bias voltage of 200 kV. Sample preparation involved deposition of the nanoparticles dispersed in $CCl_4$ onto a 200 mesh carbon-coated copper grid, which was placed on top of Fisherbrand filter paper to absorb excess solvent. The grid was then set aside to allow for evaporation of any residual $CCl_4$ before analysis. To collect the XPS data, we used a PHI 5700 X-ray photoelectron spectrometer equipped with a monochromatic Al K$\alpha$ X-ray source ($h\nu = 1486.7$ eV) incident at 90° relative to the axis of a hemispherical energy analyzer. The spectrometer was operated at high resolution with a pass energy of 23.5 eV, a photoelectron takeoff angle of 45° from the surface, and an analyzer spot diameter of 1.1 mm. Each of the samples was initially dispersed in $CCl_4$, spotted onto a gold-coated silicon wafer, and allowed to evaporate to dryness before introduction into the ultrahigh vacuum (UHV) chamber. The FTIR data were collected using a Nicolet MAGNA-IR 860 spectrometer using two separate procedures. In the first procedure, samples were dispersed in $CCl_4$, placed into a ZnSe liquid IR cell, and scanned 16 times at a spectral resolution of 1 $cm^{-1}$. In the second procedure, samples were deposited onto a polished silicon wafer, and the $CCl_4$ was allowed to evaporate before analysis. The Raman data were collected using a Nicolet Magna-IR 560 E.S.P. spectrometer equipped with a Raman module. Samples were dispersed in $CCl_4$ and subjected to 100 scans at a spectral resolution of 4 $cm^{-1}$. UV−vis spectra were collected using a Varian CARY 50 Scan UV−Visible spectrometer over the range from 300 to 1100 nm. All samples were dispersed in ethanol and loaded into a quartz cell for analysis.

**Preparation of Silica Nanoparticles.**[21] An aliquot (3.0 mL) of ammonia (30% $NH_3$ as $NH_4OH$ assay) was added to 50.0 mL of absolute ethanol. The mixture was stirred vigorously, and a subsequent aliquot (1.5 mL, 6.7 mmol) of $Si(OC_2H_5)_4$ (tetraethyl orthosilicate, TEOS) was added dropwise. Previous studies have shown that there is usually a concentration-dependent induction period required to form the $SiO_2$ nucleus from the TEOS monomer.[37] For the concentrations employed here, the induction period was approximately 30 min as judged by the change of the solution from clear to opaque white. On the basis of previous work from our laboratories,[18] the concentration of the resultant silica nanoparticles was $\sim 7 \times 10^{12}$ particles/mL. Analysis by TEM indicated that the silica nanoparticles were spherical in shape with ~100 nm diameters (data not shown).

**Functionalization of Silica Nanoparticle Surfaces with APTMS.** With the approximate concentration and surface area of the silica nanoparticles known, the amount of APTMS needed

(12) Duff, D. G.; Baiker, A. *Langmuir* **1993**, *9*, 2301.
(13) Baker, A.; Usher, F. L. *Trans. Faraday Soc.* **1940**, *36*, 385, 549.
(14) Duff, D. G.; Baiker, A.; Edwards, P. P. *J. Chem. Soc., Chem. Commun.* **1993**, 96.
(15) Schmid, G.; Lehnert, A. *Angew. Chem., Int. Ed. Engl.* **1989**, *28*, 780.
(16) Brust, M.; Walker, M.; Bethell, D.; Schiffrin, D. J.; Whyman, R. *J. Chem. Soc., Chem. Commun.* **1994**, 801.
(17) Brust, M.; Fink, J.; Bethell, D.; Schiffrin, D. J.; Kiely, C. J. *J. Chem. Soc., Chem. Commun.* **1995**, 1655.
(18) Westcott, S. L.; Oldenberg, S. J.; Lee, T. R.; Halas, N. J. *Langmuir* **1998**, *14*, 5396.
(19) In an effort to boost the initial coverage of gold, we treated silica nanoparticles with chloro(tetrahydrothiophene)gold(I), which has been shown to react with modified silica surfaces in a manner that leads to a well-distributed high coverage of gold atoms.[20,21] Upon reaction with the amino-modified silica surfaces, the tetrahydrothiophene is displaced, leaving a gold salt attached to the surface. In our hands, this strategy failed to afford growth of the metal shell, perhaps due to the fact that there is a required minimum particle size necessary to nucleate metal growth.[12,22] Alternatively, it is possible that the gold atoms are sterically shielded, which prevents the nucleation process.
(20) Slany, M.; Bardajf, M.; Casanove, M.-J.; Caminade, A.-M.; Majoral, J.-P.; Chaudret, B. *J. Am. Chem. Soc.* **1995**, *117*, 9764.
(21) Lange, P.; Schier, A.; Schmidbaur, H. *Inorg. Chem.* **1996**, *35*, 637.
(22) Kreibig, U.; Volmer, M. *Optical Properties of Metal Clusters*; Springer-Verlag: New York, 1995.
(23) Weisbecker, C. S.; Meritt, M. V.; Whitesides, G. M. *Langmuir* **1996**, *12*, 3763.
(24) Porter, Jr., L. A.; Ji, D.; Westcott, S. L.; Graupe, M.; Czernuszewicz, R. S.; Halas, N. J.; Lee, T. R. *Langmuir* **1998**, *14*, 7378.
(25) Chen, S.; Murray, R. W. *Langmuir* **1999**, *15*, 66.
(26) Shon, Y.-S.; Gross, S. M.; Dawson, B.; Porter, M.; Murray, R. W. *Langmuir* **2000**, *16*, 6555.
(27) Zamborini, F. P.; Gross, S. M.; Murray, R. W. *Langmuir* **2001**, *17*, 481.
(28) Lee, P. C.; Meisel, D. *J. Phys. Chem.* **1982**, *86*, 3391.
(29) Xu, H.; Tseng, C.-H.; Vickers, T. J.; Mann, C. K.; Schlenoff, J. B. *Surf. Sci.* **1994**, *311*, L707.
(30) Leff, D. V.; Brandt, L.; Heath, J. R. *Langmuir* **1996**, *12*, 4723.
(31) Brown, K. R.; Natan, M. J. *Langmuir* **1998**, *14*, 726.
(32) Ingram, R. S.; Hostetler, M. J.; Murray, R. W.; Schaaff, T. G.; Khoury, J. T.; Whetten, R. L.; Bigioni, T. P.; Guthrie, D. K., First, P. N. *J. Am. Chem. Soc.* **1997**, *119*, 9279.
(33) Green, S. J.; Stokes, J. J.; Hostetler, M. J.; Pietron, J.; Murray, R. W. *J. Phys. Chem. B* **1997**, *101*, 2663.
(34) Schon, G.; Simon, U. *Colloid Polym. Sci.* **1995**, *273*, 101.
(35) Ingram, R. S.; Hostetler, M. J.; Murray, R. W. *J. Am. Chem. Soc.* **1997**, *119*, 9175.
(36) Van Erp, R.; Gribnau, T. C. J.; Van Sommeren, A. P. G.; Bloemers, H. P. J. *J. Immunoassay* **1990**, *11*, 31.
(37) Iler, R. K. *The Chemistry of Silica*; Wiley: New York, 1979.

for surface functionalization can be estimated.[18,38] Consequently, we added an excess of APTMS (~50 μL, 0.28 mmol) to a 100 mL aliquot of the vigorously stirred silica nanoparticle solution and allowed the mixture to react for 2 h. The functionalization reaction could be monitored visually by ceasing stirring and observing the separation of the solution into two layers: the APTMS-coated silica nanoparticles precipitated to the bottom, leaving a clear ethanolic solution at the top. To enhance covalent bonding of the APTMS groups to the silica nanoparticle surface,[38,39] the solution was gently refluxed for 1 additional hour. The APTMS-coated silica nanoparticles were purified by centrifuging and redispersing in ethanol. Analysis of the purified nanoparticles by TEM showed no discernible difference between pre- and postfunctionalization with APTMS (data not shown).

**Preparation of Colloidal Gold Nanoparticles.**[12] To a 45 mL aliquot of HPLC grade water was added 0.5 mL of 1 M NaOH and 1 mL of THPC solution (prepared by adding 12 μL (0.067 mmol) of 80% THPC in water to 1 mL of HPLC grade water). The reaction mixture was stirred for 5 min with a strong vortex in the reaction flask. After the allotted time, 2.0 mL (27 mmol) of 1% $HAuCl_4$ in water was added quickly to the stirred solution. By variation of the volume of 1% $HAuCl_4$ added, the size of the gold colloid particles could be varied. For example, a change from 2.0 mL to 1.5 mL led to a reduction in the diameter of the nanoparticles from 2−3 nm to 1−2 nm (data not shown); the latter particles were near the detection limit of our TEM. Dried samples of the gold nanoparticles were dark brown in color, similar to that of $Au_{55}$ clusters.[12] In the work described below, we utilized colloidal gold particles that were 2−3 nm in diameter, which were routinely obtained using the procedure outlined above.

**Attachment of Colloidal Gold Nanoparticles to APTMS−Functionalized Silica Cores.**[18] An aliquot of APTMS-functionalized silica nanoparticles dispersed in ethanol (0.5 mL, ~$7 \times 10^{12}$ particles/mL) was placed in a centrifuge tube along with an excess of gold nanoparticles (5 mL of gold colloid solution, ~$7 \times 10^{14}$ particles/mL).[18] The centrifuge tube was shaken gently for a couple of minutes and then allowed to sit for 2 h. The mixture was then centrifuged at 2000 revolutions/min, and a red-colored pellet was observed to settle to the bottom of the tube. The supernatant was decanted, leaving a slightly red-colored pellet, which was redispersed and sonicated in HPLC grade water. The purified Au/APTMS/silica nanoparticles were then redispersed in 5 mL of HPLC grade water and used as described in the following subsection.

**Growth of Gold Nanoshells.** To grow the gold overlayer on the Au/APTMS/silica nanoparticles, we first had to prepare a suitable solution containing a reducible gold salt.[29] In a reaction flask, we dissolved 25 mg (0.18 mmol) of potassium carbonate ($K_2CO_3$) in 100 mL of HPLC grade water. After 10 min of stirring, 1.5 mL (20 mmol) of a solution of 1% $HAuCl_4$ in water was added. The solution initially appeared transparent yellow and slowly became colorless over the course of 30 min. To a vigorously stirred 4 mL aliquot of the colorless solution, we injected 200 μL of the solution containing the Au/APTMS/silica nanoparticles. We then added a 10 μL (0.36 mmol) aliquot of formaldehyde. Over the course of 2−4 min, the solution changed from colorless to blue, which is characteristic of nanoshell formation. The nanoshells were centrifuged and redispersed in HPLC grade water until use.

**Adsorption of Normal Alkanethiols onto Gold Nanoshells.** In a typical procedure, the gold nanoshells were centrifuged and redispersed in ethanol five times prior to exposure to solutions containing the selected alkanethiols. Solutions of three separate alkanethiols in ethanol (2 mM) were prepared: dodecanethiol, hexadecanethiol, and octadecanethiol ($C_nSH$, $n = 12$, 16, and 18, respectively). Aliquots (25 mL) of each of the thiol solutions were placed in separate flasks and vigorously stirred. To each of the thiol solutions was added 25 mL ($3.5 \times 10^{11}$ particles/mL) of bare gold nanoshells dispersed in ethanol. Each flask was covered and allowed to stir overnight. The individual samples of $C_nSH$-functionalized nanoshells were then centrifuged and redispersed five times in ethanol to remove any unreacted reagents.

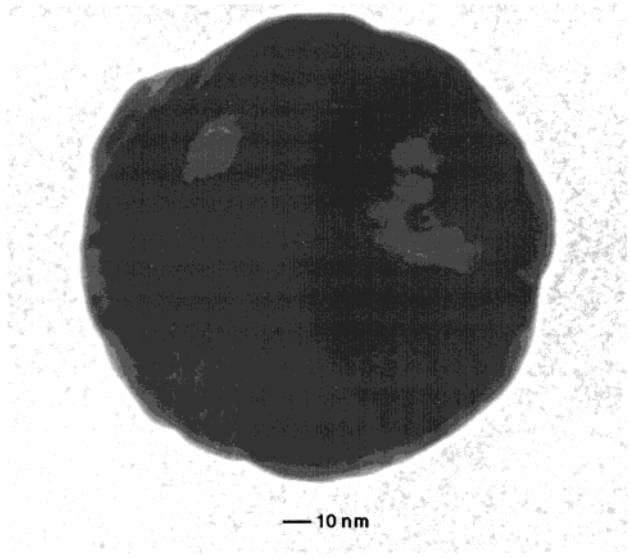


**Figure 1.** TEM image of a gold nanoshell having a silica core diameter of ~100 nm and a gold shell thickness of ~30 nm.

## Results and Discussion

**Imaging of Gold Nanoshells by TEM.** As described above, we attached small colloidal particles of gold to an APTMS-functionalized silica nanoparticle core and then used the attached gold particles to template the growth of a gold overlayer. Figure 1 shows a typical TEM image of a gold nanoshell produced using this strategy. The imaged nanoshell consists of a silica nanoparticle core having a diameter of ~100 nm encased by a gold layer having a thickness of ~30 nm. The image shows that the gold coating is continuous with topographical roughness on the nanometer scale in which the maximum difference in height between the peaks and the valleys is ~8 nm. To coat the nanoshell surfaces with SAMs, samples of nanoshells similar to the one shown here were dispersed in ethanol and added to an ethanolic solution of alkanethiol as described in the Experimental Section. While the growth of the SAM coating was undetectable by TEM, we were able to demonstrate the presence of the SAM coating through the various studies described in the following paragraphs.

**Solubility of SAM-Coated Gold Nanoshells.** The solubility of metal nanoparticles in various solvents can be used to probe the formation of SAMs on their surfaces.[24] On gold nanoparticles, the alkyl chains of alkanethiol-based SAMs extend outward from the nanoparticles, enhancing their solubility in nonpolar aprotic solvents (e.g., hexane) but not in water; in contrast, bare gold nanoparticles are soluble in water but insoluble in nonpolar aprotic solvents. We prepared several samples of alkanethiol-treated nanoshells, centrifuged them, decanted the solvent, and attempted to redisperse them in the following solvents: pentane, hexane, benzene, $CCl_4$, $CH_2Cl_2$, THF, ethanol, and water. First, the alkanethiol-treated nanoparticles could not be redispersed in water. Second, while it was possible to redisperse them in $CCl_4$ and in ethanol, the nanoshells began to precipitate from these solvents over the course of a few hours. Third, when the alkanethiol-treated nanoshells were redispersed in pentane, hexane, benzene, $CH_2Cl_2$, and THF, they remained dissolved in solution even after 48 h. Collectively,

(38) Waddell, T. G.; Leyden, D. E.; DeBello, M. T. *J. Am. Chem. Soc.* **1981**, *103*, 5303.

(39) van Blaaderen, A.; Vrij, A. J. *J. Colloid Interface Sci.* **1993**, *156*, 1.

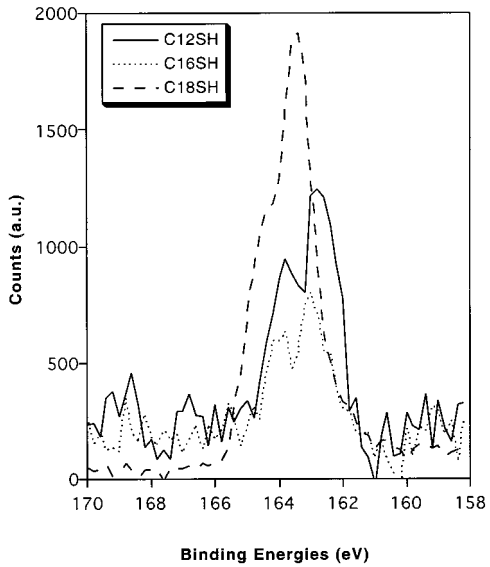


**Figure 2.** XPS scans of the S $2p_{3/2}$ region of SAM-coated gold nanoshells deposited on a gold-coated silicon wafer. The variation in signal intensity arises predominantly from differences in the number density of the nanoshells.

these observations are consistent with the formation of alkanethiol SAMs on the surfaces of the gold nanoshells.

**XPS Analysis of SAM-Coated Gold Nanoshells.** X-ray photoelectron spectroscopy is a method well-suited for the analysis of SAMs because it provides insight regarding the atomic composition of the SAM and the underlying substrate as well as information regarding the nature of the S−Au interactions.[8,23,40] Survey spectra showed only the presence of C, S, and Au (data not shown). In particular, no silicon or oxygen was detected, which is consistent with complete coverage of the silica core by the overlying gold shell. Another focus of concern regarding the functionalized nanoshells centered on evaluating the presence of free thiols versus bound thiols on the gold nanoshell surfaces.[40] The S $2p_{3/2}$ signal corresponding to either bound or free thiol appears as a doublet with a split of 1.2 eV between the peaks. For all three alkanethiol-functionalized gold nanoshells, the S $2p_{3/2}$ binding energies were less than 164 eV (Figure 2), which is consistent with sulfur bound to the surface of gold.[24,40] For unbound thiols, one would expect to see a doublet near 164 eV; in all three alkanethiol samples, however, the binding energies appeared at ∼163 eV, which was slightly higher than expected by ∼0.5−1.0 eV. We attribute the higher-than-expected binding energy to minute charging of the particles during analysis (even when using the neutralizer). The $C_{18}SH$-functionalized nanoshell exhibited the highest binding energy of the three thiols examined, followed by $C_{16}SH$ and then $C_{12}SH$. While the correlation between binding energy and chain length can perhaps be attributed to the greater insulating effects of SAMs composed of longer chain alkanethiols,[41] it is also possible that the differences arise from an experimental artifact due to differential charging of the individual samples. The absence of any oxidized sulfur species, which are typically observed at ∼166 eV,[41] is consistent with the absence of oxygen in the survey spectra described above. Overall, the XPS data were comparable to those observed for normal alkanethiol SAMs on flat gold surfaces.

**FTIR Analysis of Alkanethiol-Functionalized Gold Nanoshells.** Infrared spectroscopy offers a wealth of information regarding the structure of SAMs on flat surfaces[42−45] and on the surfaces of nanoparticles.[17,24,30,35,46,47] In particular, IR spectroscopy affords insight into the order and packing of the alkyl chains extending away from the surface. There are, for example, characteristic band positions and intensities for the C−H symmetric and antisymmetric stretches, which can offer insight into the conformational order and orientation of the alkyl chains of SAMs.[42−45] Polyethylene serves as a useful liquid and/or crystalline model for the methylene backbones of hydrocarbon SAMs.[48] When dissolved in solution, the antisymmetric $\nu_{as}(CH_2)$ bands and the symmetric $\nu_s(CH_2)$ bands appear at 2928 and 2856 $cm^{-1}$, respectively. In crystalline form, however, the bands appear at $\nu_{as}(CH_2) = 2920\ cm^{-1}$ and $\nu_s(CH_2) = 2850\ cm^{-1}$. We have found that the $\nu_{as}(CH_2)$ band is a particularly sensitive probe of conformational order.[45]

FTIR spectra of bare and SAM-coated gold nanoshells were collected using two different methodologies: (i) with the nanoshells dispersed in $CCl_4$ and (ii) with the nanoshells deposited onto a silicon wafer. For the purpose of illustration, FTIR spectra of the former samples are provided in Figure 3; the band positions are specified in Table 1. The spectra in Figure 3 show readily observable C−H stretching bands only for the SAM-coated nanoshells. Furthermore, the data in Table 1 show that when dissolved in $CCl_4$, the $\nu_{as}(CH_2)$ band of the SAM-coated nanoshells appeared at relatively high wavenumbers (e.g., 2926 $cm^{-1}$) characteristic of liquidlike packing of the methylene chains with many gauche defects.[42−48] In contrast, the data in Table 1 show that when the SAM-coated nanoshells were deposited onto a silicon wafer and the solvent was allowed to evaporate, the band positions moved to significantly lower wavenumbers (e.g., $\nu_{as}(CH_2) = 2919\ cm^{-1}$) characteristic of highly crystalline (or conformationally ordered) alkyl chains.[42−48] Also, the width of the bands in the spectra decreased upon switching from solution to the solid state, which is also consistent with an increase in crystallinity.[42−48] These trends were observed for all three of the alkanethiols studied.

This increase in crystallinity can arise from either interdigitation of the tail groups of alkyl chains attached to neighboring nanoshells or the loss of solvent molecules from the interchain matrixes of individual nanoshells.[24] Given the relative size of the nanoshells vs that of the molecules in the SAM coating, interdigitation can plausibly occur only for a fraction of the surface, even if the nanoshells were densely packed in the solid state. Furthermore, previous studies of SAM-coated colloidal gold particles also showed no evidence for interdigitation in solid-state samples.[24] These considerations lead us to conclude that the increase in crystallinity arises from the loss of solvent molecules from the SAM itself, although

(40) Johnson, S. R.; Evans, S. D.; Mahon, S. W.; Ulman, A. *Langmuir* **1997**, *12*, 51.
(41) Castner, D. G.; Hinds, K.; Grainger, D. W. *Langmuir* **1996**, *12*, 5083.
(42) Nuzzo, R. G.; Fusco, F. A.; Allara, D. L. *J. Am. Chem. Soc.* **1987**, *109*, 2358.
(43) Porter, M. D.; Bright, T. B.; Allara, D. L.; Chidsey, C. E. D. *J. Am. Chem. Soc.* **1987**, *109*, 3559.
(44) Nuzzo, R. G.; Dubois, L. H.; Allara, D. L. *J. Am. Chem. Soc.* **1990**, *112*, 558.
(45) Shon, Y.-S.; Lee, S.; Colorado, Jr., R.; Perry, S. S.; Lee, T. R. *J. Am. Chem. Soc.* **2000**, *122*, 7556.
(46) Hostetler, M. J.; Stokes, J. J.; Murray, R. W. *Langmuir* **1996**, *12*, 3604.
(47) Hostetler, M. J.; Wingate, J. E.; Zhong, C.-J.; Harris, J. E.; Vachet, R. W.; Clark, M. R.; Londono, J. D.; Green, S. J.; Stokes, J. J.; Wignall, G. D.; Glish, G. L.; Porter, M. D.; Evans, N. D.; Murray, R. W. *Langmuir* **1998**, *14*, 17.
(48) Snyder, R. G.; Strauss, H. L.; Elliger, C. A. *J. Phys. Chem.* **1982**, *86*, 5145.

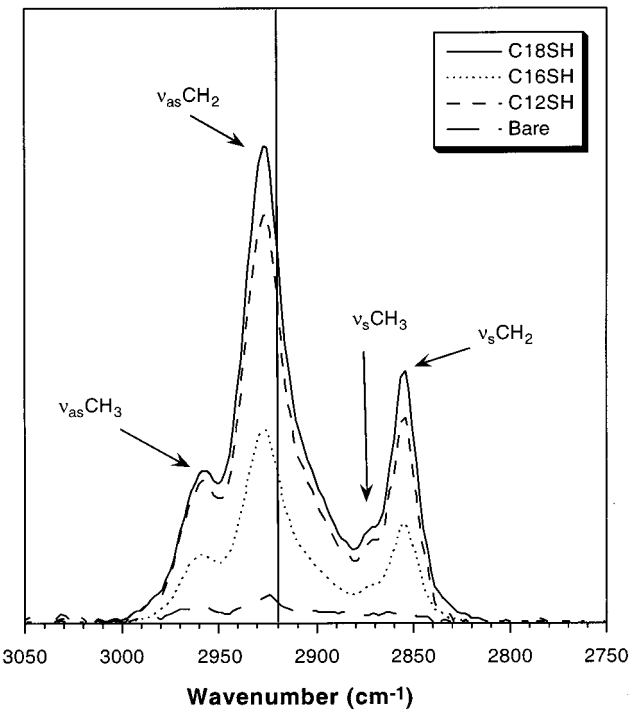


**Figure 3.** FTIR spectra of the C−H stretching region for gold nanoshells dispersed in $CCl_4$. The vertical line at 2920 $cm^{-1}$ is included for reference. The variation in signal intensity for the SAM-coated samples arises from differences in the concentration of the nanoshells.

**Table 1. Band Position ($cm^{-1}$) of the Methylene C−H Stretches of SAM-Coated Gold Nanoshells Either Dissolved in $CCl_4$ or Deposited on a Si Wafer**

| SAM | medium | $\nu_s(CH_2)$ | $\nu_{as}(CH_2)$ |
|---|---|---|---|
| $C_{12}SH$ | $CCl_4$ | 2854.7 | 2926.4 |
| $C_{16}SH$ | | 2854.7 | 2926.8 |
| $C_{18}SH$ | | 2854.7 | 2926.6 |
| $C_{12}SH$ | Si wafer | 2850.2 | 2918.7 |
| $C_{16}SH$ | | 2848.7 | 2919.1 |
| $C_{18}SH$ | | 2849.0 | 2918.3 |

previous studies have suggested the absence of residual solvent in normal alkanethiol SAMs on flat gold surfaces.[49]

**Raman Analysis of Alkanethiol-Functionalized Gold Nanoshells.** As described in the previous section, analysis of the $\nu(CH_2)$ bands by FTIR spectroscopy provides insight regarding the conformational order of the alkyl chains of SAMs. Since, however, the $\nu$(C−C) bands are weak or almost undetectable by FTIR, little information can be gleaned by IR analysis of the C−C region.[50] In contrast, Raman spectroscopy can readily detect symmetrical bonds, such as for those found in the C−C backbones of SAMs. Furthermore, for alkanethiol SAMs, analysis of the C−S and S−H bands by Raman spectroscopy provides structural and chemical insight into the interaction between the adsorbate and the underlying metal substrate.[28,29,50]

Upon chemisorption to gold, the S−H bond of alkanethiols is cleaved.[50] Thus, by examining the relative intensity of the $\nu$(S−H) band in free thiol and thiol/nanoshell samples, the adsorption step can be monitored. Figure 4 shows the $\nu$(S−H) region of the Raman spectrum of free dodecanethiol as well as that of the corresponding dodecanethiol-functionalized nanoshells. The free thiol

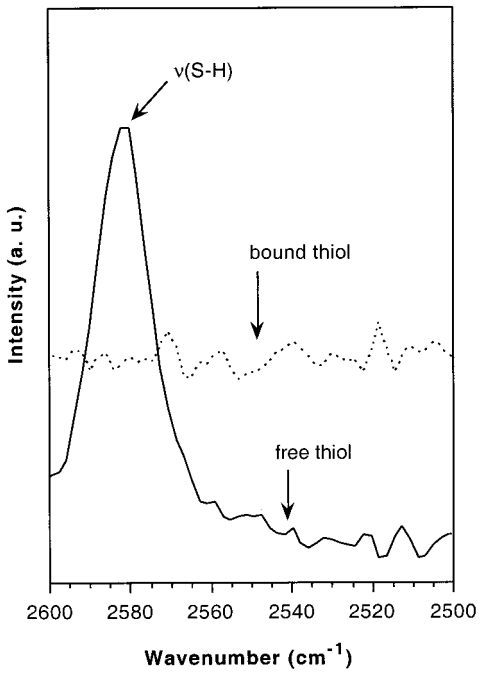


**Figure 4.** Raman spectra of the $\nu$(S−H) region for a bulk sample of dodecanethiol (solid line) and a gold nanoshell coated with dodecanethiol (dotted line).

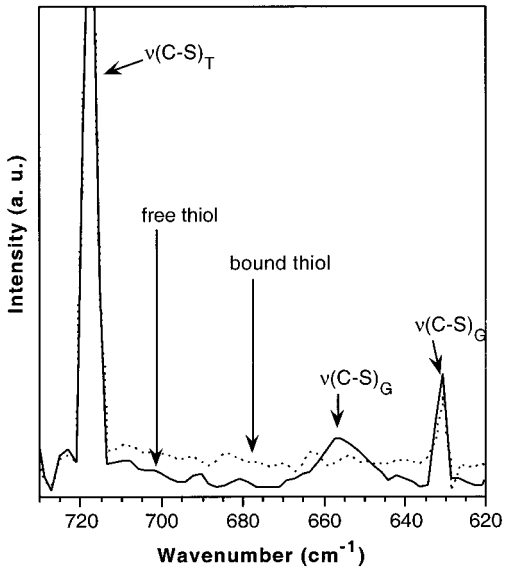


**Figure 5.** Raman spectra of the $\nu(C-S)_G$ and $\nu(C-S)_T$ regions for a bulk sample of dodecanethiol (solid line) and a gold nanoshell coated with dodecanethiol (dotted line).

exhibits a characteristic band at 2575 $cm^{-1}$; in contrast, the nanoshell sample exhibits no detectable bands in this region of the spectrum. We observed the same behavior for samples utilizing hexadecanethiol and octadecanethiol (data not shown). These observations are consistent with the chemisorption of the thiols to the surface of the gold nanoshells.[50]

Analysis of the $\nu$(C−S) region can be used to probe further the attachment process and the resultant structure of the alkyl chains near the surface of gold.[50,51] Figure 5 shows that upon going from free dodecanethiol to bound dodecanethiol, the $\nu(C-S)_G$ band at 655 $cm^{-1}$ disappears, which suggests a loss of gauche defects upon adsorption.

(49) Ulman, A.; Eilers, J. E.; Tillman, N. *Langmuir* **1989**, *5*, 1147.
(50) Bryant, M. A.; Pemberton, J. E. *J. Am. Chem. Soc.* **1991**, *113*, 8284.
(51) Sandroff, C. J.; Garoff, S.; Leung, K. P. *Chem. Phys. Lett.* **1983**, *96*, 547.

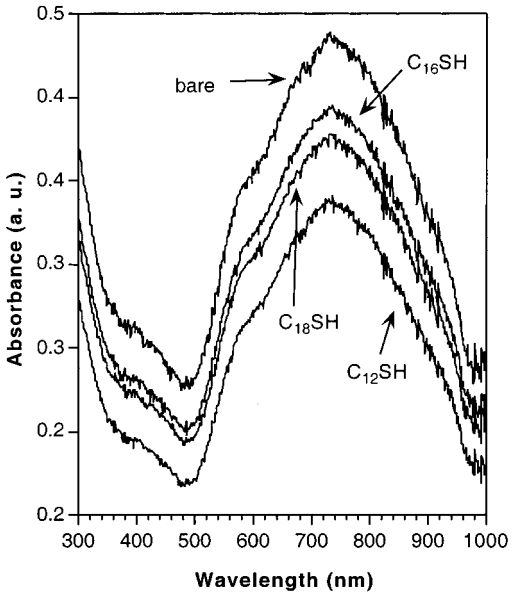


**Figure 6.** UV−vis spectra of bare, $C_{12}SH$-, $C_{16}SH$-, and $C_{18}SH$-coated gold nanoshells ($3.5 \times 10^{11}$ particles/mL) dispersed in ethanol.

These observations are consistent with ordered packing of the alkyl chain near the sulfur headgroup when the thiol attaches to the surface of the nanoshell. A prominent $\nu(C-S)_T$ band at ~715 $cm^{-1}$ arising from the predominant trans conformation of the alkyl chains is detectable both in solution and in the adsorbed films.

Additional structural insight is afforded by analysis of the $\nu(C-C)$ bands (data not shown). For the sample of liquid dodecanethiol, the $\nu(C-C)_T$ band appeared at 1120 $cm^{-1}$. In the three functionalized nanoshell samples, however, the $\nu(C-C)_T$ band shifted to higher wavenumber at ~1130 $cm^{-1}$. The gauche band, $\nu(C-C)_G$, shifted from 1075 $cm^{-1}$ as free thiol to 1065 $cm^{-1}$ as bound thiol. These observations are consistent with an enhanced trans content of the alkyl chains upon formation of a well-packed monolayer film.[24,50]

**UV−vis Spectra of Alkanethiol-Functionalized Gold Nanoshells.** Theoretical calculations have shown that the plasmon resonance of noble metal nanoshells can vary over hundreds of nanometers.[1] The position of the resonance is dictated by both the shell thickness and the size of the dielectric core. As a rule of thumb, thick shells around small cores give rise to resonances in the visible region, while thin shells around large cores give rise to resonances in the infrared region. Given that the plasmon resonance of noble metals is further sensitive to the medium in contact with the surface of the metal,[3] we wished to examine the influence of SAM adsorption upon the plasmon resonance of gold nanoshells. To this end, we employed UV−vis spectroscopy at wavelengths ranging from 300 to 1100 nm to analyze the optical absorbances of bare and SAM-coated nanoshells derived from a common batch. Figure 6 shows that for approximately equal concentrations in ethanol, all samples exhibited similar absorbance features with values of $\lambda_{max}$ at 728 nm, which is shifted by ~200 nm toward the infrared when compared to simple gold nanoparticles.[1] Given the invariance of the spectra from sample to sample, we conclude that the adsorption of normal alkanethiols onto the nanoshell surfaces exerts no strong influence upon the plasmon resonance.

## Conclusions

The exposure of gold nanoshells to a series of normal alkanethiols afforded SAM-coated gold nanoshells. The SAM coating rendered the nanoshells soluble in a wide range of organic solvents, including nonpolar aprotic solvents such as pentane, hexane, and benzene. The SAM-coated nanoshells exhibited FTIR spectra and XPS binding energies comparable to those of related SAM-coated colloidal gold particles. The XPS analyses also confirmed the integrity of the gold overlayer and showed no surface contaminants or oxidized species. Analysis by Raman spectroscopy provided strong evidence of the chemisorption of the sulfur atom to the surface of gold. Furthermore, the Raman spectra suggested an enhanced ordering of the methylene groups of the alkanethiols upon adsorption to the nanoshell surface. Analysis of the SAM-coated nanoshells by XPS, FTIR, Raman, and UV−vis spectroscopies showed no major differences for nanoshells coated with alkanethiols having three different chain lengths (i.e., $C_{12}SH$, $C_{16}SH$, and $C_{18}SH$). Furthermore, analysis by UV−vis spectroscopy showed that the plasmon resonance of gold nanoshells is unaffected by the SAM coating. Current efforts in our laboratories are targeting the use of SAMs to enhance the durability of nanoshells and to facilitate the incorporation of nanoshells into polymer matrixes.

**Acknowledgment.** We thank the Army Research Office and the Robert A. Welch Foundation for financial support.

LA015561Y